MEaSUREs Multi-year Reference Velocity Maps of the Antarctic Ice Sheet, Version 1

USER GUIDE

How to Cite These Data

As a condition of using these data, you must include a citation:

Rignot, E., B. Scheuckl, J. Mouginot, and S. Jeong. 2022. *MEaSUREs Multi-year Reference Velocity Maps of the Antarctic Ice Sheet, Version 1*. [Indicate subset used]. Boulder, Colorado USA. NASA National Snow and Ice Data Center Distributed Active Archive Center. https://doi.org/10.5067/FB851ZIZYX5O. [Date Accessed].

FOR QUESTIONS ABOUT THESE DATA, CONTACT NSIDC@NSIDC.ORG

FOR CURRENT INFORMATION, VISIT https://nsidc.org/data/NSIDC-0761

National Snow and Ice Data Center

TABLE OF CONTENTS

1 DATA DESCRIPTION 2
1.1 Parameters 2
1.2 File Information 2
1.2.1 Format 2
1.2.2 File Contents 2
1.2.3 Naming Convention 3
1.3 Spatial Information 4
1.3.1 Coverage 4
1.3.2 Resolution 5
1.3.3 Geolocation 5
1.4 Temporal Information 6
1.4.1 Coverage 6
1.4.2 Resolution 6
2 DATA ACQUISITION AND PROCESSING 6
2.1 Acquisition 6
2.2 Processing 8
2.3 Quality, Errors, and Limitations 8
2.4 Instrumentation 10
3 RELATED DATA SETS 11
4 RELATED WEBSITES 11
5 CONTACTS AND ACKNOWLEDGMENTS 11
5.1 Investigators 11
5.2 Acknowledgements 11
6 REFERENCES 12
7 DOCUMENT INFORMATION 13
7.1 Publication Date 13
7.2 Date Last Updated 13

1 DATA DESCRIPTION

This data set, part of the NASA Making Earth System Data Records for Use in Research Environments (MEaSUREs) Program, consists of three as-complete-as-possible mosaic maps of velocities on the entire Antarctic ice sheet for the time periods 1995–2001, 2007–2009, and 2014–2017. Velocities are derived via phase analysis and speckle tracking of satellite synthetic aperture radar (SAR) data as well as feature tracking of visible imagery obtained by the Operational Land Imager (OLI) on board Landsat-8.

In addition to ice velocity, the data set provides mean velocity standard error and standard deviation; counts of velocity estimates used per pixel; start and end dates for input data of each pixel; and a mask that contains the locations of ice fronts and grounding lines for each period.

1.1 Parameters

X and y component ice velocities (m/y); x and y component velocity standard error; standard deviation of velocity in x, y direction

1.2 File Information

1.2.1 Format

This data set is provided in Network Common Data (NetCDF4) (.nc) format using CF-1.6 conventions.

1.2.2 File Contents

The NetCDF4 files in the dataset contain the variables described in Table 1.

Table 1. Variable Names and Descriptions

Variable Name	Description	Fill Value	Data Type
CNT	Count of image pairs used in each pixel	0.0	float
DATE_SAMPLING_START	Start date (decimal years) of the time coverage for each pixel	0.0	float
DATE_SAMPLING_END	End date (decimal years) of the time coverage for each pixel	0.0	float
ERRX	Standard error of mean velocity in the x direction (m/y)	0.0	float
ERRY	Standard error of mean velocity in the y direction (m/y)	0.0	float

Variable Name	Description	Fill Value	Data Type
MASK	0=ocean; 1=grounded; 2=floating	N/A	byte
STDX	Standard deviation of velocity in the x direction (m/y)	0.0	float
STDY	Standard deviation of velocity in the y direction (m/y)	0.0	float
VX	Ice velocity in the x direction (m/y)	0.0	float
VY	Ice velocity in the y direction (m/y)	0.0	float
crs	Coordinate reference system details	N/A	char
lat	Latitude	N/A	double
lon	Longitude	N/A	double
x	Cartesian x coordinate (m)	N/A	double
y	Cartesian y coordinate (m)	N/A	double

Note: To convert the VX and VY ice velocity components into magnitude (speed) and direction (angle), as well as their relative errors, use the following equations (Mouginot et al., 2012):

- speed = sqrt (VX^2 + VY^2)
- angle = arctan (VY / VX)
- error = sqrt ($ERRX^2$ + $ERRY^2$)
- error of flow direction = error / (2*speed)

When computing the inverse tangent, users should take note of the function's inherent ambiguities. While the standard arctan function typically does not account for angles that differ by 180°, most modern computer languages and math software packages include the function ATAN2, which uses the signs of both vector components to place the angle in the proper quadrant.

1.2.3 Naming Convention

This data set comprises the following three data files, with the corresponding date range specified in the file name:

- antarctica_ice_velocity_1995-2001_450m_v01.0.nc
- antarctica_ice_velocity_2007-2009_450m_v01.0.nc
- antarctica_ice_velocity_2014-2017_450m_v01.0.nc

1.3 Spatial Information

1.3.1 Coverage

The dataset spans the Antarctic ice sheet (see Figure 1 for exact coverage from the various sensors used to create the dataset):

- Southernmost Latitude: 90° S
- Northernmost Latitude: 60° S
- Westernmost Longitude: 180° W
- Easternmost Longitude: 180° E

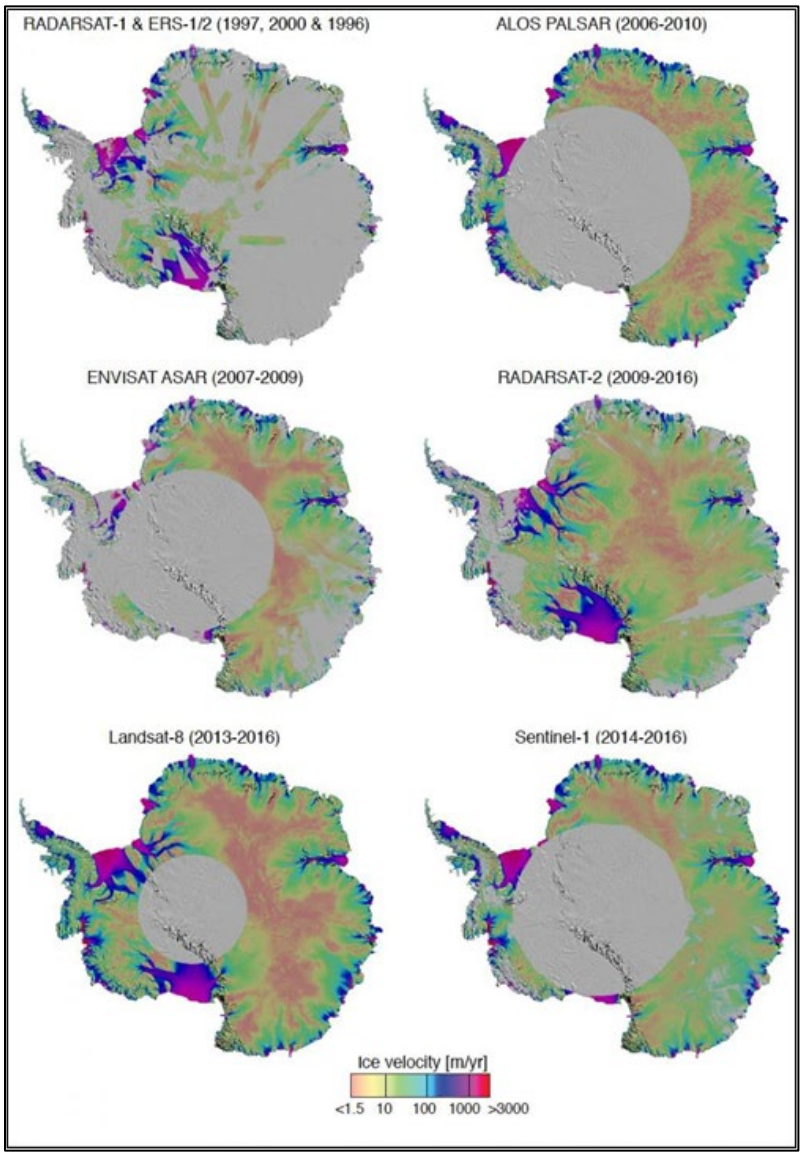

Figure 1. Antarctic ice velocity derived from RADARSAT-1, ERS-1 and 2, ALOS PALSAR, ENVISAT ASAR, RADARSAT-2, Landsat-8, and Sentinel-1, color-coded on a logarithmic scale and overlaid on a MODIS mosaic of Antarctica. Projection is polar stereographic at 71° S secant plane.

1.3.2 Resolution

The spatial resolution of the ice velocity map is 450 m by 450 m.

1.3.3 Geolocation

The data are provided in the WGS 84/Antarctic Polar Stereographic projection. The following tables provide information for geolocating this data set:

Table 2. Geolocation Details

Geographic coordinate system	WGS 84
Projected coordinate system	WGS 84 / Antarctic Polar Stereographic
Longitude of true origin	0
Latitude of true origin	-71
Scale factor at longitude of true origin	1
Datum	WGS_1984
Ellipsoid/spheroid	WGS 84
Units	meter
False easting	0
False northing	0
EPSG code	3031
PROJ4 string	+proj=stere +lat_0=-90 +lat_ts=-71 +lon_0=0 +k=1 +x_0=0 +y_0=0 +datum=WGS84 +units=m +no_defs
Reference	https://epsg.io/3031

Table 3. Grid Details

Grid cell size (x, y pixel dimensions)	450 m x 450 m
Number of rows	12445
Number of columns	12445
Geolocated lower left point in grid	54.67353057861328° S, 225.0° E
Nominal gridded resolution	450 m
Grid rotation	N/A
ulxmap – x-axis map coordinate of the center of the upper-left pixel (XLLCORNER for ASCII data)	-2799775.0
ulymap – y-axis map coordinate of the center of the upper-left pixel (YLLCORNER for ASCII data)	2799775.0

1.4 Temporal Information

1.4.1 Coverage

The time periods represented by each of the three time series maps were selected to maximize spatial coverage and minimize error compared to annual maps, while still restricting the observation period (for an annual map see MEaSUREs Annual Antarctic Ice Velocity Maps 2005-2017):

- 01 July 1995 to 30 June 2001
- 01 July 2007 to 30 June 2009
- 01 July 2014 to 30 June 2017

1.4.2 Resolution

Varies (see Coverage section above and Table 4. Satellite/Sensor Data Ranges below)

2 DATA ACQUISITION AND PROCESSING

2.1 Acquisition

Table 4 outlines the satellites and sensors used to acquire this data and their specifications.

Table 4. Temporal and spatial coverage of source satellite data

Platform/Sensor	**Space Agency**	**Look Dir.**	**Mode**	**Repeat Cycle *(day)***	**Incidence Angle**	**Resolution *Rg x Az (m)***	**Frequency *(GHz)***	**Year**
ERS-1 & 2/SAR	European Space Agency (ESA)	Right	N/A	1-3	23	13x4	5.33	1996
RADARSAT-1/SAR	Canadian Space Agency (CSA)	Left/Right	Varies	24	18-47	12x5-17x6	5.33	1997/2000
ENVISAT/ASAR	ESA	Right	IS2	35	23	13x5	5.33	2007-2009
RADARSAT-2/SAR	CSA	Left	S5/EH4	24	41/57	12x5	5.33	2009-2017
ALOS/PALSAR	Japan Aerospace Exploration Agency (JAXA)	Right	FBS	46	39	7x4	1.27	2006-2010
ALOS-2/PALSAR-2	Japan Aerospace Exploration Agency (JAXA)	Left/Right	Varies	14	8-70	1x3	1.26	2014-2017
Sentinel-1/SAR	ESA	Right	IW-T OPS	12		12x43	5.33	2014-2017
Landsat-8/OLI	USGS/NASA	N/A	Panchromatic	16	N/A	15x15		2013-2017
TanDEM-X/TerraSAR-X/SAR	German Space Agency (DLR)	Right	N/A	11	46.3	1.4x1.8	9.65	2011-2017

The temporal periods included in each of the three maps coincide with acquisition campaigns. During the 1996-2000 period, RADARSAT-1 acquired data with the Antarctic Mapping Mission (AMM) in 1997 and the Modified Antarctic Mapping Mission (MAMM) in late 2000 while ERS-1/2 acquired data in coastal Antarctica in 1996. The 2007-2009 and 2014-2017 periods include data collected as part of the International Polar Year (IPY) campaign and Polar Space Task Group's acquisitions respectively.

2.2 Processing

Ice velocities were derived from a variety of SAR data sources using a number of interferometric analysis techniques, including:

- Combining interferometric phases from two independent tracks to retrieve the surface flow vector (Mouginot et al., 2019)
- Augmenting the phase map in coastal areas with speckle tracking in both along-track (azimuth) and across-track (range) directions (Rignot et al., 2011; Mouginot et al., 2012; Mouginot et al., 2017)
- Calculating two-dimensional offsets in amplitude imagery (Mouginot et al., 2012)
- Combining range interferometric phases along two independent tracks (Mouginot et al., 2012)

In all cases, surface parallel flow is assumed, a conventional approach for ice sheets. The Landsat-8 data are processed using repeat image feature tracking (see Mouginot, et al. 2017).

2.3 Quality, Errors, and Limitations

A detailed description of these data and their quality is provided in Rignot, et al., 2011, Mouginot, et al., 2014, and Mouginot, et al., 2017. The precision of ice flow mapping varies with the sensor, the geographic location, the technique of interferometric analysis (see Data Acquisition and Processing section above), the time period of analysis, the repeat cycle, and the amount of data stacking. Table 5 provides the error in ice velocity mapping for each sensor, without data stacking, in range (Rg) and azimuth (Az).

- The error map in Figure 2 takes into account the following error sources:
- Error of speckle tracking and interferometric phase analysis respectively (SAR only)
- Errors caused by ionospheric perturbations (strongest in the azimuth direction, stronger in L-band compared to C-band, stronger in the East Antarctic ice sheet (EAIS) compared to the West Antarctic ice sheet (WAIS) because ionospheric perturbations are more abundant near the magnetic pole)
- Error of feature tracking analysis (Landsat-8 only)
- Data stacking (reduces the error noise as the square root of the number of interferometric pairs averaged)

- Respective weight of each instrument in the mosaicking

The total error is the square root of the sum of the independent errors squared. More details on the error estimates are provided in Mouginot, et al., 2017.

Table 4. Error in Ice Velocity Mapping (m/yr)

Platform/Sensor	Nominal Repeat Cycle (day)	Error (m/yr)	
		Rg	Az
ALOS (WAIS)/PALSAR	46	6	17
ALOS (EAIS)/PALSAR	46	6	5
ENVISAT/ASAR	35	21	4
RADARSAT-2/SAR	24	26	8
RADARSAT-1/SAR	24	26	8
Sentinel-1/SAR	12	12	43
Landsat-8/OLI	16	34[1]	34[1]
TanDEM-X (TDX)/TerraSAR-X (TSX)/SAR	11	8	8
Tandem ERS-1 and -2 (phase)/SAR	1	1	N/A

[1]Landsat uses repeat image feature tracking in x and y

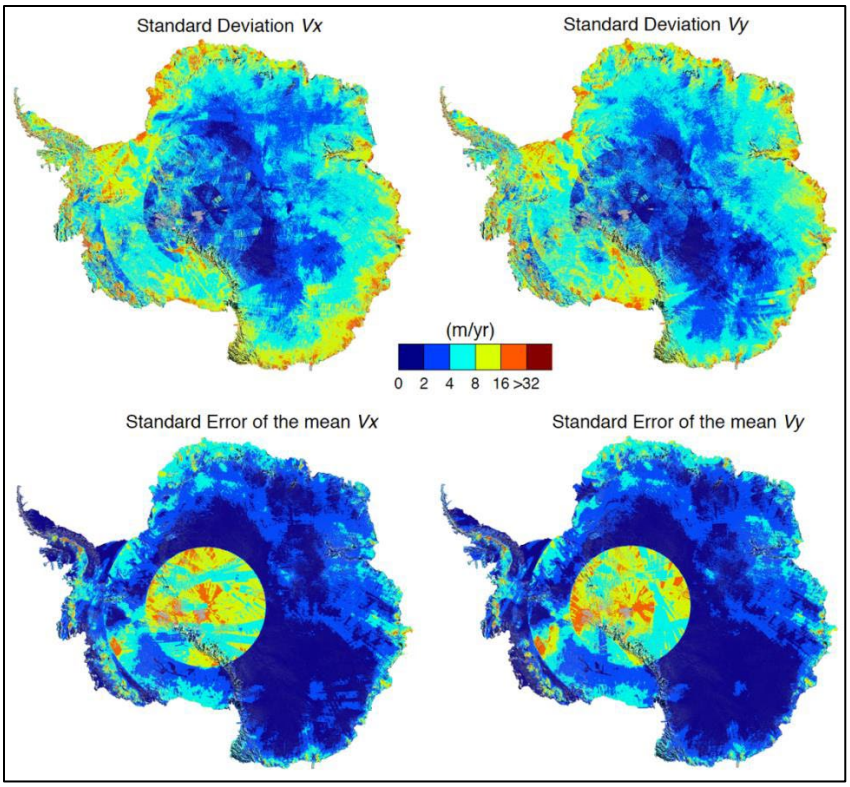

Figure 2. Standard deviation of vx and vy (top row) and standard error of the mean vx and vy on a linear scale color-coded from 1 to greater than 32 m/yr.

2.4 Instrumentation

For more information about the missions, satellites, and instruments used to create this data set, see the following websites:

The European Space Agency

- ERS Instruments (ERS-1, -2)
- RADARSAT Instruments (RADARSAT- 1, -2)
- ENVISAT Instruments (ASAR)
- Sentinel Online | Instrument Payload (Sentinel-1)
- TerraSAR-x and TanDEM-X Instruments

Alaska Satellite Facility

- ALOS PALSAR

U.S. Geological Survey

- Landsat-8 (OLI)

3 RELATED DATA SETS

MEaSUREs InSAR-Based Antarctica Ice Velocity Map

MEaSUREs Phase-Based Antarctica Ice Velocity Map

MEaSUREs Annual Antarctic Ice Velocity Maps 2005-2017

MEaSUREs Antarctic Grounding Line from Differential Satellite Radar Interferometry

MEaSUREs BedMachine Antarctica

MEaSUREs InSAR-Based Ice Velocity of the Amundsen Sea Embayment, Antarctica

MEaSUREs Antarctic Boundaries for IPY 2007-2009 from Satellite Radar

4 RELATED WEBSITES

MEaSUREs Data | Overview

5 CONTACTS AND ACKNOWLEDGMENTS

5.1 Investigators

Eric Rignot, Bernd Scheuchl, Jeremie Mouginot, and Seongsu Jeong
Department of Earth System Science
Croul Hall
University of California, Irvine
Irvine, CA 92697
USA

5.2 Acknowledgements

These data were generated through a grant from the NASA MEaSUREs program.

Spaceborne Synthetic Aperture Radar (SAR) acquisitions were provided through the following data agencies:

- ALOS PALSAR: Japan Aerospace Exploration Agency (JAXA)
- ENVISAT ASAR, ERS-1, ERS-2: European Space Agency (ESA)
- Sentinel-1: Copernicus/ESA
- RADARSAT-1, RADARSAT-2: Canadian Space Agency (CSA)
- TerraSAR-X, TanDEM-X: German Aerospace Center(DLR)
- Landsat-8 (optical) data: United States Geological Survey (USGS).

Data acquisitions between 2006 and 2016 are courtesy of the International Polar Year (IPY) Space Task Group and its successor, the Polar Space Task Group (PSTG).

Contains modified Copernicus Sentinel-1 data (2014-2016), acquired by the ESA, distributed through the Alaska Satellite Facility, and processed by Rignot, E, J. Mouginot, and B. Scheuchl.

The TanDEM-X DEM of Antarctica is courtesy of DLR.

6 REFERENCES

Li, X., Rignot, E., Mouginot, J., & Scheuchl, B. (2016). Ice flow dynamics and mass loss of Totten Glacier, East Antarctica, from 1989 to 2015. *Geophysical Research Letters*, *43*(12), 6366–6373. doi: 10.1002/2016GL069173.

Michel, R., & Rignot, E. (1999). Flow of Glaciar Moreno, Argentina, from repeat-pass Shuttle Imaging Radar images: Comparison of the phase correlation method with radar interferometry. *Journal of Glaciology*, *45*(149), 93–100. doi: 10.3189/S0022143000003075.

Mouginot, J., Rignot, E., & Scheuchl, B. (2014). Sustained increase in ice discharge from the Amundsen Sea Embayment, West Antarctica, from 1973 to 2013. *Geophysical Research Letters*, *41*(5), 1576–1584. doi: 10.1002/2013GL059069.

Mouginot, J., Rignot, E., & Scheuchl, B. (2019). Continent-Wide, Interferometric SAR Phase, Mapping of Antarctic Ice Velocity. *Geophysical Research Letters*, *46*(16), 9710–9718. doi: 10.1029/2019GL083826.

Mouginot, J., Rignot, E., Scheuchl, B., & Millan, R. (2017). Comprehensive annual ice sheet velocity mapping using Landsat-8, Sentinel-1, and RADARSAT-2 data. *Remote Sensing*, *9*(4), 364. doi: 10.3390/rs9040364.

Mouginot, J., Scheuchl, B., & Rignot, E. (2012). Mapping of ice motion in Antarctica using Synthetic-Aperture Radar data. *Remote Sensing*, *4*(9), 2753–2767. doi: 10.3390/rs4092753.

Rignot, E., Bamber, J. L., van den Broeke, M. R., Davis, C., Li, Y., van de Berg, W. J., & van Meijgaard, E. (2008). Recent Antarctic ice mass loss from radar interferometry and regional climate modelling. *Nature Geoscience*, *1*(2), 106–110. doi: 10.1038/ngeo102.

Rignot, E., Jacobs, S., Mouginot, J., & Scheuchl, B. (2013). Ice-shelf melting around Antarctica. *Science*, *341*(6143), 266–270. doi: 10.1126/science.1235798.

Rignot, E., Mouginot, J., & Scheuchl, B. (2011a). Antarctic grounding line mapping from differential satellite radar interferometry: *Geophysical Research Letters*, *38*(10). doi: 10.1029/2011GL047109.

Rignot, E., Mouginot, J., & Scheuchl, B. (2011b). Ice flow of the Antarctic ice sheet. *Science*, *333*(6048), 1427–1430. doi: 10.1126/science.1208336.

Rignot, E., Mouginot, J., Scheuchl, B., van den Broeke, M., van Wessem, M. J., & Morlighem, M. (2019). Four decades of Antarctic ice sheet mass balance from 1979–2017. *Proceedings of the National Academy of Sciences*, *116*(4), 1095–1103. doi: 10.1073/pnas.1812883116.

Scheuchl, B., Mouginot, J., & Rignot, E. (2012). Ice velocity changes in the Ross and Ronne sectors observed using satellite radar data from 1997 and 2009. *The Cryosphere*, *6*(5), 1019–1030. doi: 10.5194/tc-6-1019-2012.

7 DOCUMENT INFORMATION

7.1 Publication Date

October 2022

7.2 Date Last Updated

October 2022